Research Square

Preprints are preliminary reports that have not undergone peer review.
They should not be considered conclusive, used to inform clinical practice,
or referenced by the media as validated information.

Trunk-directed airflow reduces mediolateral postural sway during tandem stance

Tianyi Wang

gmwangtianyi@gmail.com

The University of Osaka https://orcid.org/0000-0001-8066-6408

Shinichi Yoshimura

Takafumi Ohno

Yuko Ohno

Article

Keywords: postural control, tandem stance, airflow, center of pressure, rambling–trembling decomposition, sensory cue

Posted Date: November 6th, 2026

DOI: https://doi.org/10.21203/rs.3.rs-11591493/v1

License: This work is licensed under a Creative Commons Attribution 4.0 International License.
Read Full License

Additional Declarations:
There is **NO** Competing Interest.

Informed consent was obtained from all participants.

Trunk–directed airflow reduces mediolateral postural sway during tandem stance

Abstract

The postural control system can use sensory cues to regulate body orientation; however, whether noncontact airflow contributes to stance control remains unclear. Here, we show that airflow directed at the trunk alters postural variability during tandem stance. Ten healthy young adults completed three 30 sec trials in each of three conditions (no airflow, continuous airflow, and 60–Hz pulsed airflow) while center–of–pressure (CoP) signals were recorded. Linear mixed–effects model showed lower mediolateral CoP variability during 60–Hz airflow than during no airflow (estimated difference, 1.42 mm; Holm–adjusted $p = 0.021$), with no significant difference between the two airflow conditions. Rambling–trembling decomposition localized the clearest change to the mediolateral rambling component; its standard deviation and range were lower during 60–Hz airflow than during no airflow. Airflow also shortened the time to the minimum of the CoP velocity–direction correlation curve. These findings indicate that trunk–directed airflow can influence postural control without physical contact and motivate further study of how airflow–induced cutaneous cues are incorporated into multisensory balance control.

Keywords: postural control, tandem stance, airflow, center of pressure, rambling–trembling decomposition, sensory cue

1 Introduction

Human upright stance is maintained through continuous feedback between body motion and sensory information from the visual, vestibular, and somatosensory systems. When the reliability of one sensory source changes, the nervous system can alter the relative contributions of other sensory signals to stabilize the body. This sensory reweighting is a central feature of models of human postural control and provides a framework for understanding how additional sensory information may be incorporated into balance regulation [1, 2].

A well–established example is light touch. A fingertip contact force that is too small to provide meaningful mechanical support can nevertheless reduce postural sway, indicating that contact can provides spatial information about body orientation that is used by the postural control system [3, 4]. Passive tactile stimulation applied to the leg, shoulder, and finger can also reduce sway without active touch; this effect is

particular apparent when visual or plantar sensory information is limited [5–7] These observations show that the postural system can exploit externally available tactile information even the stimulus does not physically support body. Related studies using subsensory mechanical noise applied to the feet have shown that stochastic stimulation can improve balance, providing a complementary example of sensory augmentation [8, 9].

Airflow is a potentially useful but distinct form of external input because it can deform the skin without physical contact. This possibility has received some attention in previous research. Backlund Wasling et al. reported that a thin air stream could reduce postural sway when applied to glabrous skin and examined its value as a source of spatiotemporal tactile information [10]. However, their study focused on cutaneous directional sensitivity and compared airflow with a skin–stretch stimulus on the forearm and fingertip. Whether airflow directed at the trunk modulates postural control during a mechanically constrained stance and whether any such modulation is expressed selectively in particular directions or components of postural sway remain unresolved.

To address this question, we delivered airflow to the waist of adults standing in tandem stance with their eyes closed. Tandem stance markedly narrows the mediolateral base of support, increasing the biomechanical challenge to lateral postural control [11, 12]. Therefore, we examined whether trunk–directed airflow was associated with reduced mediolateral sway and whether any effect was preferentially expressed in the rambling rambling component of the center–of–pressure (CoP) trajectory. Rambling–trembling decomposition separates CoP fluctuations into a rambling component, which reflects the migration of an instantaneous equilibrium reference, and a trembling component, which describe oscillations around that reference [13, 14]. Previous studies have shown that these components can respond differently to change in the base of support, although their neural interpretations remains inferential rather than direct [15]. In addition, we quantified the temporal organization of sway using a direction–change measure based on the cosine of the angle between velocity vectors separated in time [16].

This study compared three conditions: no airflow, continuous airflow, and airflow pulsed at 60 Hz. Because the physical characterization showed that the two airflow conditions had different dominant oscillatory components, we treated them as distinct stimulus conditions rather than as a test of whether 60 Hz is intrinsically optimal. We hypothesized that trunk–directed airflow would reduce postural variability during tandem stance and that any effect would be most apparent in the mechanically constrained mediolateral direction. We further examined whether airflow–related changes would preferentially involve the rambling rather than the trembling component and whether the timing of directional reversal would be altered.

2 Results

2.1 Airflow stimuli differed in temporal structure

A custom pneumatic system delivered airflow horizontally to the lower trunk through a nozzle positioned approximately 20 cm from the waist. In the continuous condition, the

airflow valve remained open, whereas in the pulsed condition, the valve was switched at 60 Hz (Fig. 1). A vibration sensor placed 20 cm from the nozzle was used to characterize the stimulus delivered at the experimental distance. The two airflow conditions produced similar peak sensor amplitudes (approximately ± 0.07 mV) but different frequency spectra. The pulsed condition showed a dominant 60–Hz component, whereas the nominally continuous condition showed a dominant 120–Hz component, which was attributed to the dual–piston compressor. Thus, the two airflow conditions differed in both temporal modulation and dominant mechanical oscillation (Fig. 2).

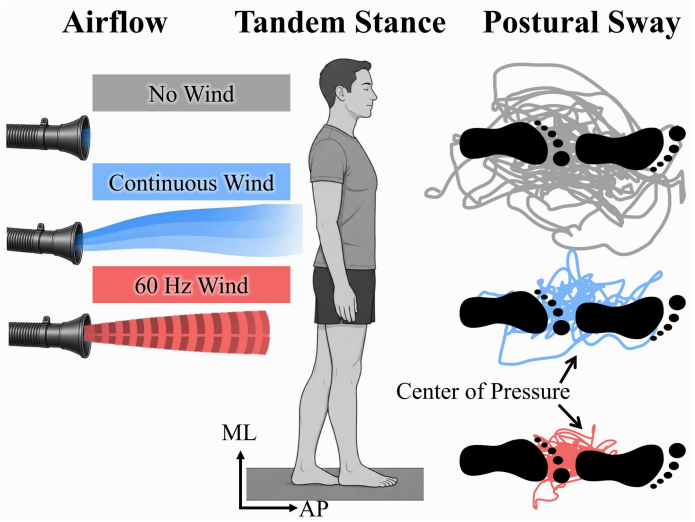


Fig. 1 Experimental concept and airflow conditions. Three conditions were applied to the lower trunk during tandem stance: no airflow, continuous airflow, and 60–Hz pulsed airflow. The force–plate coordinate system is shown with the anteroposterior (AP) and mediolateral (ML) directions. The figure is a schematic of the study setup and not a mechanistic model.

This characterization is important for interpretation because the present experiment did not isolate a frequency–specific effect at 60 Hz. Any difference between the two airflow conditions must therefore be attributed to the difference between the complete physical stimuli produced by the two delivery modes.

2.2 Trunk–directed airflow reduced mediolateral postural variability

Participants stood in the tandem stance with their eyes closed for three 30–sec trials in each condition, with the condition order randomized. The primary outcome measure was the standard deviation of CoP displacement in the mediolateral direction (SD_{ML}). A linear mixed–effects model with condition as a fixed effect and participant–specific random intercepts revealed a significant overall effect of condition on SD_{ML} ($F_{2,78} = 4.10$, $p = 0.020$).

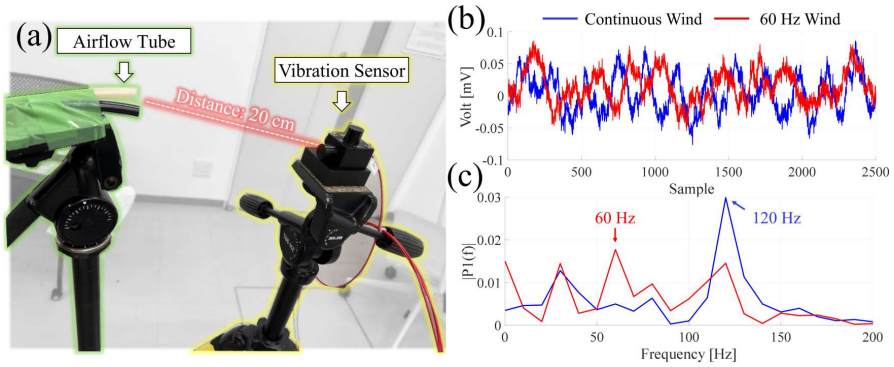


Fig. 2 Physical characterization of the delivered airflow stimuli. Representative time–domain sensor traces and single–sided amplitude spectra for continuous and 60–Hz pulsed condition. The pulsed condition showed a dominant 60–Hz component, whereas the nominally continuous condition showed a dominant 120–Hz component associated with compressor pulsation.

The model–estimated SD_{ML} decreased from 9.18 mm in the no–airflow condition to 8.16 mm during continuous airflow and 7.76 mm during 60–Hz airflow (Fig. 3 (a)) The estimated difference between no airflow and 60–Hz airflow was 1.42 mm (95%CI, 0.40–2.43 mm; Holm–adjusted $p = 0.021$). The no–airflow versus continuous airflow contrast was smaller (1.02 mm) and did not survive Holm correction ($p = 0.098$), and the two airflow conditions did not differ (0.40 mm; $p = 0.439$). Thus, the data support a reduction in mediolateral variability under airflow,, with the clearest evidence arising from the 60–Hz condition relative to no airflow; however, they do not establish a difference between the two airflow conditions.

2.3 The clearest airflow–associated changes occurred in the mediolateral rambling component

Next, we examined whether the condition effect was similar expressed in the rambling and trembling components fo the mediolateral and anteroposterior CoP trajectories (Fig. 4) Condition effects were confined to the mediolateral rambling measures. For the standard deviation of the mediolateral rambling trajectory ($SD_{RM,ML}$), the omnibus condition effect was significant ($F_{2,78} = 4.60$, $p = 0.013$). The estimated marginal means were 7.29, 6.17, and 5.78 for no airflow, continuous airflow, and 60–Hz airflow, respectively (Fig. 3 (b)). The no airflow versus 60–Hz contrast was 1.51 (Holm–adjusted $p = 0.014$), whereas the no airflow versus continuous airflow contrast was 1.12 ($p = 0.066$); the two airflow conditions did not differ significant ($p = 0.457$).

A similar pattern was observed for the range of the mediolateral rambling trajectory ($Range_{RM,ML}$; Fig. 3 (c)). The estimated marginal means decreased from 39.28 during no airflow to 32.02 during continuous airflow and 29.63 during 60–Hz airflow (condition effect: $F_{2,78} = 4.11$, $p = 0.020$). The no airflow versus 60–Hz contrast was 9.65 (Holm–adjusted $p = 0.022$); the corresponding contrast for continuous airflow was 7.26 ($p = 0.083$), and the two airflow conditions did not differ ($p = 0.498$).

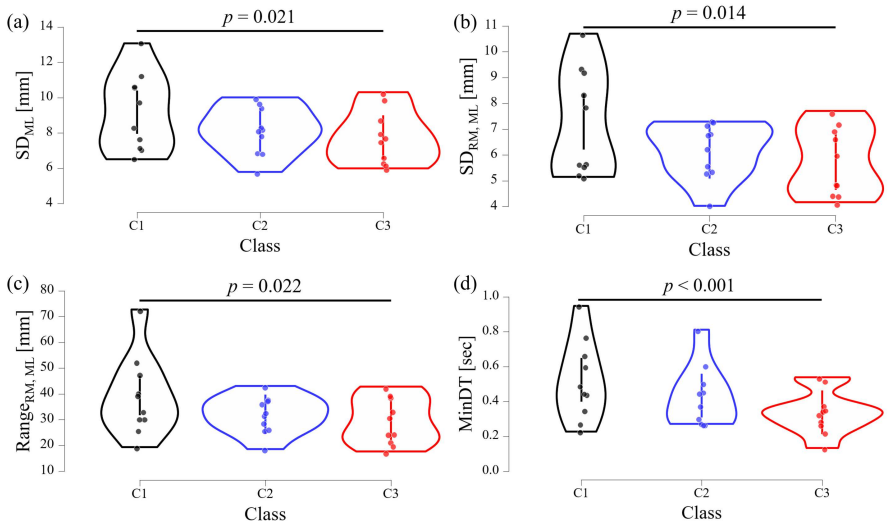


Fig. 3 Key outcome measures across airflow conditions. Participant–level distributions of the four key outcomes reported in the main text: (a) standard deviation of mediolateral CoP displacement (SD_{ML}); (b) standard deviation of the mediolateral rambling trajectory ($SD_{RM,ML}$); (c) range of the mediolateral rambling trajectory ($Range_{RM,ML}$); and (d) time to the minimum of the directional correlation curve ($MinDT$).

2.4 Airflow altered the timing, but not the magnitude of the directional reversal

To characterize the temporal structure of sway, we calculated the cosine of the angle between CoP velocity vectors separated by progressively longer intervals. Three summary measures were derived: the interval at which the cosine first became negative ($ZeroCrossDT$), the minimum cosine value ($MinValue$), and the interval at which the minimum occurred ($MinDT$).

$ZeroCrossDT$ showed an overall condition effect ($F_{2,78} = 3.60$, $p = 0.032$), but none of the three Holm–corrected pairwise contrasts was significant. $MinValue$ showed no evidence of a condition effect ($F_{2,78} = 0.02$, $p = 0.976$). In contrast, $MinDT$ differed strongly across conditions ($F_{2,78} = 9.00$, $p < 0.001$); the estimated marginal means were 0.521, 0.434, and 0.338 sec under no, continuous, and 60–Hz airflow, respectively (Fig. 3 (d)). The no airflow versus 60–Hz contrast was 0.183 sec (95%CI, 0.097–0.269 sec; Holm–adjusted $p < 0.001$). The other pairwise contrasts did not survive Holm correction (both $p = 0.058$). Thus, airflow was associated with earlier timing of the strongest directional reversal, without a detectable change in the magnitude of the reversal itself.

3 Discussion

The present study shows that trunk–directed airflow is associated with reduced mediolateral postural variability during tandem stance. The effect was most clearly expressed

in the 60–Hz airflow condition relative to the no airflow condition, and component–level analysis localized the strongest changes to the mediolateral rambling trajectory rather than the trembling trajectory. A separate analysis of directional dynamics showed that the strongest reversal in CoP velocity occurred earlier with airflow, without a corresponding change in reversal magnitude. Taken together, these observations indicate that a noncontact aerodynamic stimulus can alter the organization of human postural control during a constrained stance.

These findings extend those of previous studies on the role of external sensory information in postural control. Light touch and passive cutaneous stimulation can reduce sway even when the stimulus does not provide mechanical support [3–6]. An earlier airflow study [10] established that air streams can carry behaviorally useful tactile information for postural control, particularly when applied to glabrous skin. The present study differs from that study in several respects: the stimulus was directed at the lower trunk rather than the fingertip or forearm; the task imposed a narrow mediolateral base of support; and the analysis examined both the component structure and temporal organization of CoP fluctuations. Therefore, the results provide evidence that the postural system can be influenced by airflow at the trunk during a mechanically challenging stance, although the underlying sensory pathway remains unresolved.

The concentration of the effects on the mediolateral rambling measures is consistent with the mechanical asymmetry of tandem stance. Narrowing the base of support primarily increases the demand on lateral stability, and previous experiments manipulating support geometry have reported stronger effects of mediolateral than anteroposterior instability on postural sway and its rambling–trembling components [11, 15]. However, in the present study, stance width was not directly manipulated. Therefore, the data support only a conditional statement: within tandem stance, airflow–related changes were detected most clearly in the direction that was most constrained by the task. They do not establish that airflow effects scale systematically with base–of–support width.

The rambling–trembling results also require careful interpretation. The original decomposition was introduced to distinguish the migration of an instantaneous equilibrium reference from oscillations around that reference [13, 14], and subsequent studies have shown that the two components can respond differently to changes in support geometry [15]. Nevertheless, rambling and trembling are derived from the same force plate signal and should not be treated as direct proxies for supraspinal and spinal neural activity, respectively. Therefore, the present finding that airflow effects were concentrated on rambling is consistent with a change in the organization or movement of the estimated postural reference trajectory; however, it does not identify the neural locus of that change. This distinction is important because airflow can alter both sensory input and the physical state of the trunk, either of which could influence the inferred rambling trajectory.

The directional-change analysis provides a complementary perspective. The minimum of the velocity–direction correlation curve occurred approximately 35% earlier in the 60–Hz condition than in the no airflow condition, whereas the minimum value itself was unchanged. This suggests a change in the timing of postural corrections

rather than a simple scaling of their magnitude. This measure was originally introduced to quantify directional changes in the CoP trajectory under different feedback conditions [16]; in the present study, it should likewise be interpreted as a descriptor of sway dynamics rather than as a direct measure of feedback latency. Nevertheless, the convergence of the rambling and directional–dynamics analyses suggests that airflow was associated with more than a uniform reduction in sway amplitude.

An important limitation is that the experiment did not separate the sensory and mechanical effects of airflow. Although the stimulus characterization demonstrated distinct 60–Hz and 120–Hz components, the sensor output was not calibrated directly against airflow velocity, pressure at the skin, or force on the trunk. Therefore, we could not determine whether the observed changes arose from cutaneous sensory information, direct mechanical perturbation of the trunk, or both. Similarly, this study did not quantify perceptual thresholds, skin deformation, or muscle activity. These limitations preclude a mechanistic conclusion regarding whether the effect resembles the informational contribution of light touch or the sensory enhancement proposed for stochastic resonance.

Interpretation of the 60–Hz condition also requires caution. Because the continuous condition exhibited a dominant 120–Hz component and the two airflow conditions were not significantly different from one another, the present experiment did not demonstrate a 60–Hz–specific optimum or establish that pulsed stimulation recruits a distinct receptor mechanism. The appropriate conclusion is that different airflow delivery modes produced related postural effects, with the statistical evidence occurring for 60–Hz airflow relative to no airflow. Frequency–dependent effects therefore remain a hypothesis to be tested in future experiments using independently controlled airflow intensities and waveforms.

Finally, the sample was small and restricted to healthy young adults, and only a single stance configuration was tested. Three 30–sec trials per condition were collected, which is comparable to the protocols used in conventional CoP studies but shorter than the 60–s duration recommended for some rambling–trembling measures in a reliability study [15]. Therefore, the current findings should be regarded as evidence of a reproducible within–session association in this task rather than as evidence that the effect generalizes across populations or balance conditions. A larger, independently replicated study with calibrated airflow measurements, controlled mechanical loading, and direct measures of body kinematics and muscle activity is required to establish the underlying mechanism and the generality of this effect.

Within these limitations, the data support the specific conclusion that trunk–directed airflow can modify human postural control during tandem stance without physical contact. The direction– and component–specific pattern suggests that the effect is organized around the control demands of the task rather than reflecting a simple, global increase or decrease in sway. Whether this reflects the use of airflow–derived cutaneous information as an additional postural cue is an experimentally testable question that follows directly from the present findings.

In conclusion, trunk–directed airflow altered postural dynamics during tandem stance, with the clearest evidence for reduced mediolateral CoP variability and reduced variability of the mediolateral rambling component during 60–Hz airflow relative to

no airflow. Airflow was also associated with earlier timing of the strongest directional reversal. These results indicate that a noncontact aerodynamic stimulus can influence human postural control, although the relative contributions of sensory and mechanical effects remain unresolved.

4 Methods

4.1 Participants

Ten healthy young adults (age: 22.2 ± 0.7 y.o.) participated in this study.

4.2 Experimental Setup and Airflow Stimulation

A custom pneumatic system was constructed to deliver controlled airflow horizontally to the lower trunk. A variable–frequency drive controlled the motor of an oil–free wobble–piston air pump. Compressed air was stored in a stainless–steel buffer tank before delivery through a relay–based switching element and a flexible tube to a nozzle mounted on an adjustable tripod. In the continuous condition, the relay was continuously energized. In the pulsed condition, the relay was switched at 60 Hz. In the no airflow (control) condition, the pneumatic system was inactive. The nozzle height and angle were adjusted for each participant such that the airflow was directed horizontally toward the waist (lumbar region).

Participants stood on a portable force plate in tandem stance, with one foot placed directly in front of the other in a heel–to–toe configuration along the sagittal axis, and kept their eyes closed. Each participant completed three 30–sec trials in each condition, for a total of nine trials. The trial order across conditions was randomized, and participants were given brief rest periods between trials to reduce fatigue.

4.3 Airflow Stimulus Characterization

The physical stimulus was characterized at approximately 20 cm from the nozzle, matching the experimental nozzle–to–waist distance. A vibration sensor recorded the stimulus in the time domain, and a single–sided fast Fourier transform was used to inspect its frequency content. Peak sensor amplitudes were approximately ±0.07 mV in both airflow conditions. The pulsed condition showed a dominant spectral peak at 60 Hz, whereas the nominally continuous condition showed a dominant peak at 120 Hz. These measurements were used to characterize the temporal structure of the delivered stimulus and were not interpreted as calibrated measurements of force, pressure, or airflow velocity.

4.4 Force–Plate Acquisition and CoP Processing

Ground–reaction–force data were sampled at 1200 Hz during each 30–sec trial. CoP trajectories were obtained in the anteroposterior (AP) and mediolateral (ML) directions. The CoP and horizontal shear force signals were low–pass filtered with a zero–phase, second–order Butterworth filter at 10 Hz. The primary outcome measure,

the standard deviation of ML CoP displacement (SD_{ML}), was calculated over the full trial using Eq. 1:

$$SD_{ML} = \sqrt{\frac{1}{N-1}\sum_{i=1}^{N}(ML_i - \overline{ML})^2}. \quad (1)$$

4.5 Rambling–Trembling Decomposition

The rambling (RM) and trembling (TR) trajectories were obtained from the filtered CoP and horizontal shear force signals using the instant equilibrium point (IEP) procedure described by Zatsiorsky and Duarte [13, 14]. For each direction, zero crossings of the horizontal shear force were identified by linear interpolation between adjacent samples that straddled the sign change. The CoP values at these times were interpolated using a cubic spline to reconstruct the RM trajectory. The TR trajectory was calculated as the difference between the filtered CoP and RM trajectories. Standard deviation, range, path length, and mean velocity were calculated for each RM and TR trajectory in the AP and ML directions.

The horizontal shear force vanishes precisely at the instants when the CoP coincides with the IEP:

$$F_d(t_k) = 0 \Rightarrow IEP_d(t_k) = CoP_d(t_k), d \in \{AP, ML\}. \quad (2)$$

The rambling trajectory $RM_d(t)$ was then reconstructed by cubic spline interpolation through the set of CoP values sampled at the K_d zero–crossing instants:

$$RM_d(t) = CubicSpline(\{(t_k, CoP_d(t_k))\}_{k=1}^{K_d}; t). \quad (3)$$

The trembling trajectory $TR_d(t)$ was obtained as the residual after subtracting the rambling trajectory from the original CoP signal, as follows:

$$TR_d(t) = CoP_d(t) - RM_d(t). \quad (4)$$

4.6 Directional–Change Analysis

The directional dynamics of CoP sway were quantified using the method of [16] (Fig. 5). For time intervals of up to 1 s, the cosine of the angle between velocity vectors separated by each interval was calculated and averaged across valid sample pairs. Three summary measures were derived from each resulting curve: $ZeroCrossDT$, the first interval at which the curve became negative; $MinValue$, the minimum value of the curve; and $MinDT$, the interval at which the minimum occurred.

The instantaneous velocity components were first computed from the filtered CoP signal using first–order backward differences as follows:

$$V_i = \left(\frac{P_{AP,i} - P_{AP,i-1}}{\Delta t}, \frac{P_{ML,i} - P_{ML,i-1}}{\Delta t}\right) \quad (5)$$

For a given time interval $\Delta T = n\Delta t$, where Δt is the sampling interval, the cosine of the angle between velocity vectors separated by n samples was computed as:

$$cos\theta(i, i+n) = \frac{V_{AP,i}V_{AP,i+n} + V_{ML,i}V_{ML,i+n}}{\sqrt{V_{AP,i}^2 + V_{ML,i}^2}\sqrt{V_{AP,i+n}^2 + V_{ML,i+n}^2}}, \tag{6}$$

and averaged across all valid sample pairs to obtain a single directional–persistence value for each ΔT:

$$cos\theta(\Delta T) = \frac{1}{N-n}\sum_{i=1}^{N-n} cos\theta(i, i+n). \tag{7}$$

4.7 Statistics and Reproducibility

The primary analysis tested the effect of airflow condition on SDML using a linear mixed–effects model. Condition (no airflow, continuous airflow, or 60–Hz pulsed airflow) was entered as a fixed effect, and participant identity was included as a random intercept. All three trials for each condition were retained as repeated observations, yielding 90 observations from 10 participants. Degrees of freedom were estimated using the Satterthwaite approximation. When the omnibus condition effect was significant, the three prespecified pairwise comparisons used in the original analysis were evaluated using two–sided tests with Holm adjustment. Significance level was set as $\alpha = 0.05$.

The same mixed–effects framework was applied separately to the RM/TR and directional–change measures. Importantly, Holm adjustment was applied to the three pairwise contrasts within each outcome but not across the full set of outcome measures. Therefore, the RM/TR and directional–change analyses were interpreted as mechanistic and complementary analyses rather than as independent confirmatory endpoints.

All signal processing was performed using custom MATLAB (MathWorks, Natick, MA, USA, version R2018a) scripts, and statistical analyses were performed using JASP (JASP Team, Amsterdam, the Netherlands, version 0.98.1).

References

[1] Peterka, R.J.: Sensorimotor integration in human postural control. Journal of Neurophysiology **88**(3), 1097–1118 (2002) https://doi.org/10.1152/jn.2002.88.3.1097

[2] Horak, F.B.: Postural orientation and equilibrium: what do we need to know about neural control of balance to prevent falls? Age and Ageing **35**(suppl 2), 7–11 (2006) https://doi.org/10.1093/ageing/afl077

[3] Jeka, J.J., Lackner, J.R.: Fingertip contact influences human postural control. Experimental Brain Research **100**(3), 495–502 (1994) https://doi.org/10.1007/BF02738408

[4] Clapp, S., Wing, A.M.: Light touch contribution to balance in normal bipedal stance. Experimental Brain Research **125**(4), 521–524 (1999) https://doi.org/10.1007/s002210050711

[5] Rogers, M.W., Wardman, D.L., Lord, S.R., Fitzpatrick, R.C.: Passive tactile sensory input improves stability during standing. Experimental Brain Research **136**(4), 514–522 (2001) https://doi.org/10.1007/s002210000615

[6] Menz, H.B., Lord, S.R., Fitzpatrick, R.C.: A tactile stimulus applied to the leg improves postural stability in young, old and neuropathic subjects. Neuroscience Letters **406**(1), 23–26 (2006) https://doi.org/10.1016/j.neulet.2006.07.014

[7] Shima, K., Shimatani, K., Sakata, M.: A wearable light-touch contact device for human balance support. Scientific Reports **11**(1), 7324 (2021) https://doi.org/10.1038/s41598-021-85687-4

[8] Priplata, A., Niemi, J., Salen, M., Harry, J., Lipsitz, L.A., Collins, J.J.: Noise-enhanced human balance control. Physical Review Letters **89**(23), 238101 (2002) https://doi.org/10.1103/PhysRevLett.89.238101

[9] Priplata, A.A., Niemi, J.B., Harry, J.D., Lipsitz, L.A., Collins, J.J.: Vibrating insoles and balance control in elderly people. The Lancet **362**(9390), 1123–1124 (2003) https://doi.org/10.1016/S0140-6736(03)14470-4

[10] Backlund Wasling, H., Norrsell, U., Göthner, K., Olausson, H.: Tactile directional sensitivity and postural control. Experimental Brain Research **166**(2), 147–156 (2005) https://doi.org/10.1007/s00221-005-2343-5

[11] Day, B.L., Steiger, M.J., Thompson, P.D., Marsden, C.D.: Effect of vision and stance width on human body motion when standing: implications for afferent control of lateral sway. The Journal of Physiology **469**(1), 479–499 (1993) https://doi.org/10.1113/jphysiol.1993.sp019824

[12] Mochizuki, L., Duarte, M., Amadio, A.C., Zatsiorsky, V.M., Latash, M.L.: Changes in postural sway and its fractions in conditions of postural instability. Journal of Applied Biomechanics **22**(1), 51–60 (2006) https://doi.org/10.1123/jab.22.1.51

[13] Zatsiorsky, V.M., Duarte, M.: Instant equilibrium point and its migration in standing tasks: Rambling and trembling components of the stabilogram. Motor Control **3**(1), 28–38 (1999) https://doi.org/10.1123/mcj.3.1.28

[14] Zatsiorsky, V.M., Duarte, M.: Rambling and trembling in quiet standing. Motor Control **4**(2), 185–200 (2000) https://doi.org/10.1123/mcj.4.2.185

[15] Słomka, K., Juras, G., Sobota, G., Bacik, B.: The reliability of a rambling-trembling analysis of center of pressure measures. Gait & Posture **37**(2), 210–213

(2013) https://doi.org/10.1016/j.gaitpost.2012.07.005

[16] Nagano, A., Noritake, H., Luo, Z.: An analysis of directional changes in the center of pressure trajectory during stance. Gait & Posture **31**(3), 400–402 (2010) https://doi.org/10.1016/j.gaitpost.2010.01.007

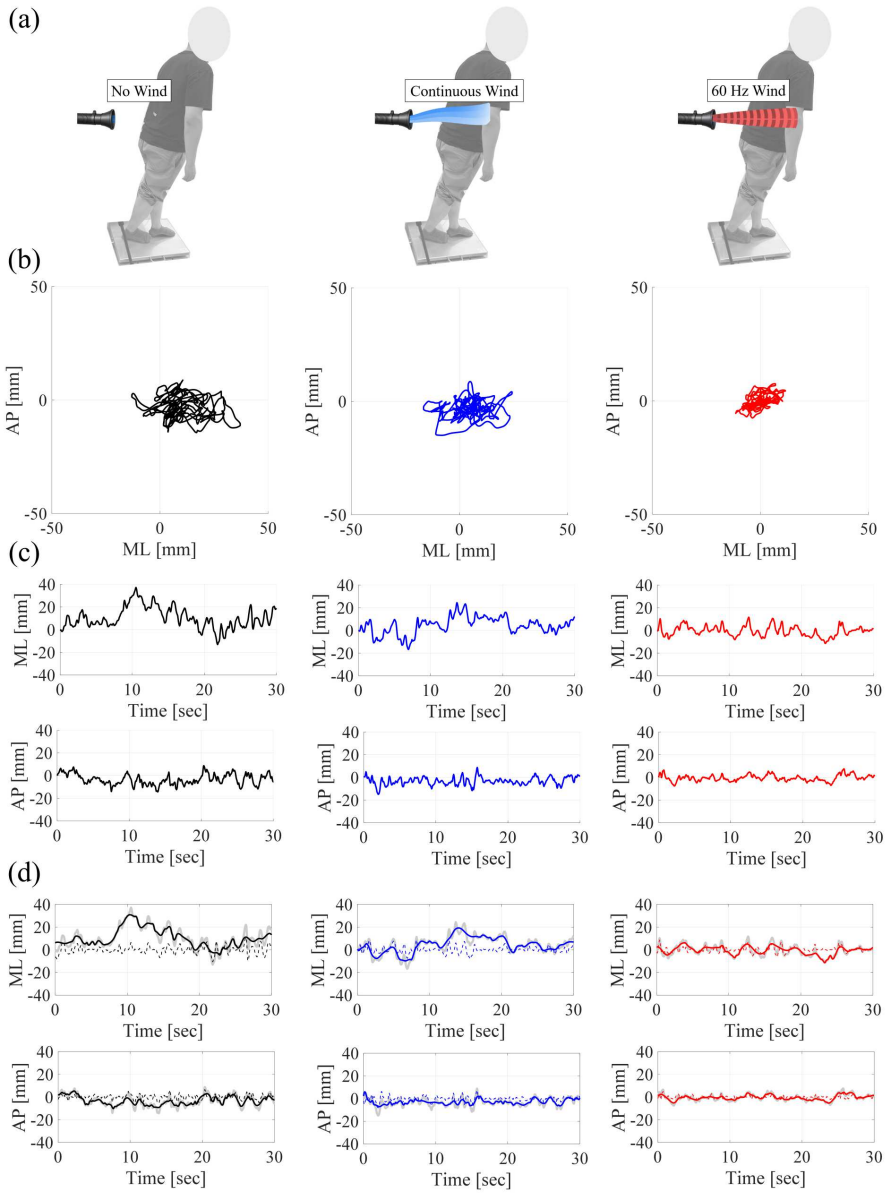


Fig. 4 Representative CoP trajectory and rambling–trembling decomposition for one participant. This example illustrates the analysis procedure.

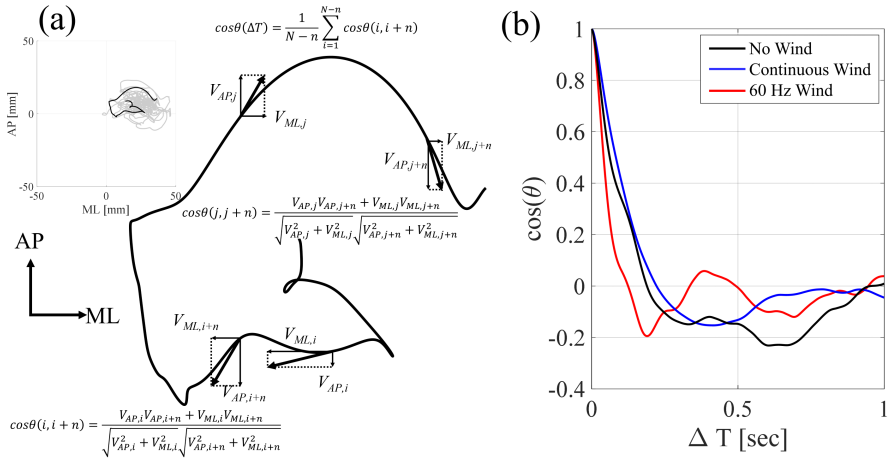


Fig. 5 Airflow changes the timing of directional reversal in postural sway. Example of the directional–correlation analysis derived from CoP velocity vectors.